Structural Engineering and Mechanics, *Vol. 71, No. 5 (2019) 553-562*
DOI: https://doi.org/10.12989/sem.2019.71.5.553

Accuracy of incidental dynamic analysis of mobile elevating work platforms

Miomir L.J. Jovanović[1a], Goran N. Radoičić[*2] and Vladimir S. Stojanović[1b]

[1]*University of Niš, Faculty of Mechanical Engineering, Str. Al. Medvedev 14, Niš 18000, Serbia*
[2]*University "Union – Nikola Tesla" Belgrade, Faculty of Applied Sciences in Niš, Str. Emp. Dušan 62-64, Belgrade 11000, Serbia*

(Received August 31, 2018, Revised April 12, 2019, Accepted April 18, 2019)

Abstract. This paper presents the results of a study into the dynamic behaviour of a support structure of a mobile elevating work platform. The vibrations of the mechanical system of the observed structure are examined analytically, numerically, and experimentally. Within the analytical examination, a simple mathematical model is developed to describe free and forced vibrations. The dynamic analysis of the mechanical system is conducted using a discrete dynamic model with a reduced number of vibrational degrees of freedom. On the basis of the expression for the system energy, and by applying Lagrange's equations of the second kind, differential equations are derived for system vibrations, frequencies are determined, and the laws of forced platform vibration are established. At the same time, a nonlinear FEM model is developed and the laws of free and forced vibration are determined. The experimental and numerical part of the study deal with the examination of the real structure in extreme conditions, taking into account: the lowest eigenfrequency, forced actions that could endanger the general stability, the maximal amplitudes, and the acceleration of the work platform. The obtained analytical and numerical results are compared with the experiments. The experimental verification points to the adverse behaviour of the platform in excitation cases – swaying. In such a situation, even a relatively small physical force can lead to unacceptably high amplitudes of displacement and acceleration – exceeding the usual work values.

Keywords: experiment; FEM; frame structures; incidental dynamic analysis; mechanical model; numerical simulation

1. Introduction

People who work at height with mobile elevating work platforms detect machine vibrations differently. However, almost everyone agrees that such work is uncomfortable and risky due to pronounced vibrations. Such a qualification emphasizes the importance of the research into the vibrations of support structures of elevating platforms. Particularly important are forced vibrations caused by incidental actions. The aim of such research is, above all, to increase the level of safety of people and reduce material damage.

Leah *et al.* (2013) analyse the incidents that occurred in the operation of elevating work platforms in a twenty-year period from 1989 to 2009. In this analysis, the incidents are classified according to the type of machine and the outcome (Table 1). The outcomes are divided into six categories: fall, overturning, trapping, injury, collapse (failure), electrocution. According to Table 1, the most common incidents are those that happen in scissor lifts (50% of the total number), followed by articulating booms (21%) and vehicle mounted booms (20%). Incidental actions, which

Table 1 MEWP incident analysis for the observed period 1989-2009 (Leah *et al.* 2013)

		Type of MEWP						
		Scissor Lift	Articulating boom	Telescopic boom	Vehicle mounted boom	Rail mounted boom	Deck mounted boom	Totals
Outcome	Falls from MEWPs	43	14	9	17	0	0	83
	MEWP overturned	53	17	5	7	0	0	82
	Trapped/crushed by MEWP	26	16	2	2	0	1	47
	Injured by MEWP	21	3	1	7	0	0	32
	Collapse/ MEWP failure	4	7	6	20	1	0	38
	Electrocution	0	3	0	5	0	0	8
	Totals	147	60	23	58	1	1	290

cause the extreme dynamics of transport machines with frame structures, are modelled in Radoičić *et al.* (2014).

Elevating work platform incidents occur in irregular modes and extreme working conditions. The problems in maintaining the stability of tall machines appear in severe external circumstances, for example, gusts of wind (Bošnjak *et al.* 2009, Radoičić 2006, Radoičić and Jovanović 2017). A significant number of incidents stem from inadequate operation (Dong *et al.* 2012, Fujioka *et al.* 2009), and even malicious intent. The occurrence of failures

*Corresponding author, Ph.D.
E-mail: goran.radoicic@gmail.com
[a] Professor
E-mail: miomir@masfak.ni.ac.rs
[b] Ph.D.
E-mail: stojanovic.s.vladimir@gmail.com

http://www.techno-press.com/journals/sem&subpage=7
ISSN: 1225-4568 (Print), 1598-6217 (Online)

Table 2 Elevating work platform CTE.Z19 - characteristics

Manufacturer:	CTE S.p.A., Italy
Type of structure:	Articulated-telescopic
Produced:	2008
Max working height:	19 m
Max working range:	8 m
Payload:	230 kg
Turret rotation:	360º
Gross weight:	3400 kg
Dimensions (safe position):	6550×2200×2900H mm
Max allowed wind speed:	12.5 m/s
Basic vehicle type:	Sprinter MB311
Vehicle engine power:	80 kW (EU4)

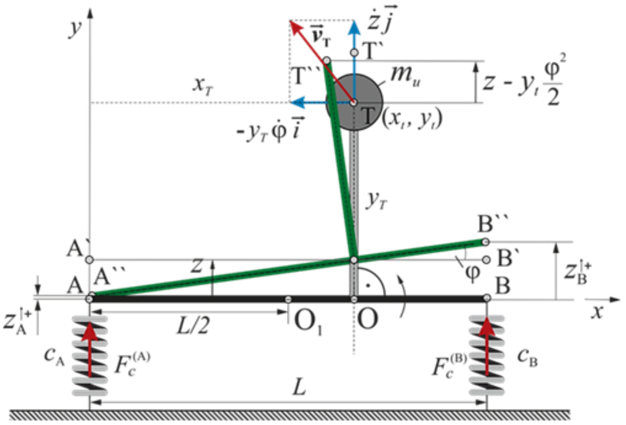

Fig. 1 Reduced dynamic MEWP model (MEWP - Mobile Elevating Work Platform)

in responsible structural elements (Bošnjak *et al.* 2015), together with frequent problems of mechanical stability, places these transport machines into a very risky group, thus making these problems a pressing research topic.

The dynamic analysis of the elevating work platform incidents was performed on the basis of the theory of small system vibrations. First, eigenvalues were determined (modal analysis) along with the behaviour of the platform as a whole when subjected to external excitation (transient analysis). The mechanical (analytical) model of the machine, developed in this paper, is discrete, with a finite number of degrees of freedom. The model is verified both numerically (FEM simulation) and experimentally, by measurement on a physical object. A vehicle mounted CTE.Z19 elevating work platform was used, with an articulated-telescopic boom and other characteristics as given in Table 2.

The operating position of the support structure was chosen for the dynamic analysis, with the machine positioned using its stabilizers onto a relatively consolidated ground (asphalt) of typical compressibility. The elasticity of the supports was taken from previous research (Radoičić *et al.* 2014, Jovanović 1990).

2. Free vibrations of the mechanical system of the elevating work platform with two vibrational degrees of freedom

The mechanical system of the elevating work platform comprises twelve important elements (masses) connected by joints. In the basic (simple) analytical model, all masses are reduced to a single concentrated mass in the point of their centre of gravity. This facilitates the mathematical analysis of the complex system (Stojanović and Kozić 2015). In such a case, the system is reduced to a single concentrated mass m_u, which is connected using a “light” bar to the platform and the immovable support with two springs of equal rigidities c_A and c_B, Fig. 1. In this way the spatial problem is reduced to a planar one. The analysis is performed in the vertical plane, where the spatial system with four springs that support the platform in the horizontal (equilibrium) position – is reduced to two, rigidities c_A and c_B (Rašković 1965). The reduced mechanical model of the platform in Fig. 1 represents a system with two vibrational degrees of freedom with the generalized coordinates $z(t)$ and $\varphi(t)$.

To determine the potential energy of the system in Fig. 1, it is necessary to first determine the static deflections of the springs f_{st1} and f_{st2} and the forces within them from the system equilibrium conditions Eqs. (1)-(2):

$$\sum_{i=1}^{3} Y_i = c_A f_{st1} + c_B f_{st2} - m_u g \tag{1}$$

$$\sum_{i=1}^{3} M_i^{O_1} = -c_A f_{st1}\frac{L}{2} + c_B f_{st2}\frac{L}{2} - m_u g\left(x_T - \frac{L}{2}\right) = 0 \tag{2}$$

By solving the system of Eqs. (1)-(2), we determine the forces in the springs in the following form:

$$F_c^{(A)} = c_A f_{st1} = \frac{m_u g\left(L - x_T\right)}{L}, F_c^{(B)} = c_B f_{st2} = \frac{m_u g x_T}{L} \tag{3}$$

The kinetic energy of the reduced system in Fig. 1 is the kinetic energy of the concentrated mass m_u, which moves at speed: $\left|\vec{v}_t\right| = \sqrt{\dot{z}^2 + \left(y_T\dot{\varphi}\right)^2}$, i.e.

$$E_k^{(s)} = E_k^{(m_u)} = \frac{1}{2} m_u \left(\dot{z}^2 + y_T^2\dot{\varphi}^2\right) \tag{4}$$

The potential energy of the system comprises the change in the potential energy of mass m_u and the potential energies of the springs, and has the form, Eq. (5)

$$\begin{aligned} E_p^{(s)} &= E_p^{(m_u)} + E_p^{(c_A)} + E_p^{(c_B)} = \\ &= m_u g\left[z - y_T\left(1 - \cos\varphi\right)\right] + \frac{1}{2} c_A\left[\left(f_{st1} - z_A\right)^2 - f_{st1}^2\right] + \\ &+ \frac{1}{2} c_B\left[\left(f_{st2} - z_B\right)^2 - f_{st2}^2\right] \end{aligned} \tag{5}$$

where

$$z_A = z - x_T\varphi, \qquad z_B = z + \left(L - x_T\right)\varphi \tag{6}$$

By substituting the obtained expressions and the expression for the static deflections of the springs from Eq. (3) into the expression for potential energy Eq. (5) (bearing in mind that what is being considered are system vibrations at small angular displacements sin$\varphi \approx \varphi$), we obtain a simplified expression for the potential energy of the system:

$$E_p^{(s)} = \frac{1}{2}\left[c_A(z-\varphi x_T)^2 + c_B(z+L\varphi-\varphi x_T)^2 - g\varphi^2 m_u y_T\right] \quad (7)$$

By sorting the coefficients according to the generalized coordinates $z(t)$ and $\varphi(t)$, the potential energy is:

$$\begin{aligned} E_p^{(s)} &= \frac{1}{2}(c_A+c_B)z^2 + \left[Lc_B - (c_A+c_B)x_T\right]z\varphi + \\ &+ \frac{1}{2}\left[c_B(L-x_T)^2 + c_A x_T^2 - g m_u y_T\right]\varphi^2 \end{aligned} \quad (8)$$

Based on the expression for the potential energy of the system Eq. (8), it can be concluded that there is a link between the generalized coordinates, conditioned by the asymmetrical geometry of the system. The application of Lagrange's equations of the second kind for conservative systems:

$$\frac{d}{dt}\frac{\partial E_k^{(s)}}{\partial \dot{z}} - \frac{\partial E_k^{(s)}}{\partial z} + \frac{\partial E_p^{(s)}}{\partial z} = 0 \quad (9)$$

$$\frac{d}{dt}\frac{\partial E_k^{(s)}}{\partial \dot{\varphi}} - \frac{\partial E_k^{(s)}}{\partial \varphi} + \frac{\partial E_p^{(s)}}{\partial \varphi} = 0 \quad (10)$$

yields a homogeneous system of two differential equations with constant coefficients in the following form

$$2a_1\ddot{z} + 2b_1 z + b_2\varphi = 0 \quad (11)$$

$$2a_2\ddot{\varphi} + 2b_3\varphi + b_2 z = 0 \quad (12)$$

where

$$\begin{aligned} &a_1 = \frac{1}{2}m_u,\ \ a_2 = \frac{1}{2}m_u y_T^2,\ \ b_1 = \frac{1}{2}(c_A+c_B), \\ &b_2 = Lc_B - (c_A+c_B)x_T, b_3 = \frac{1}{2}\left[c_B(L-x_T)^2 + c_A x_T^2 - g m_u y_T\right] \end{aligned} \quad (13)$$

When it comes to the homogeneous system of differential equations of the second kind with constant coefficients, the solution of system Eqs. (11)-(12) is assumed in the following form

$$z = Ae^{i\omega t}, \qquad \varphi = Be^{i\omega t}, \qquad i = \sqrt{-1} \quad (14)$$

where ω is the natural frequency of the small system vibrations.

By substituting solution Eq. (14) into the system of differential equations Eqs. (11)-(12), we obtain a homogeneous system of algebraic equations according to the unknown constants A and B, as follows

$$Ae^{it\omega}\left(-2\omega^2 a_1 + 2b_1\right) + Be^{it\omega}b_2 = 0 \quad (15)$$

$$Ae^{it\omega}b_2 + Be^{it\omega}\left(-2\omega^2 a_2 + 2b_3\right) = 0 \quad (16)$$

For the system of Eqs. (15)-(16) to have a nontrivial solution, it is necessary and sufficient that the system determinant according to the unknown constants A and B is equal to zero, i.e.

$$\det\begin{bmatrix} -2\omega^2 a_1 + 2b_1 & b_2 \\ b_2 & -2\omega^2 a_2 + 2b_3 \end{bmatrix} = 0 \quad (17)$$

Developing the determinant Eq. (17) yields a bi-square frequency equation in the form

$$\omega^4 - \omega^2\left(\frac{b_1}{a_1} + \frac{b_3}{a_2}\right) - \frac{b_2^2}{4a_1 a_2} + \frac{b_1 b_3}{a_1 a_2} = 0 \quad (18)$$

whose solutions are the natural frequencies of the system

$$\begin{aligned} \omega_1^2 &= \frac{4a_2 b_1 + 4a_1 b_3}{8a_1 a_2} - \\ &- \frac{\sqrt{\left(-4a_2 b_1 - 4a_1 b_3\right)^2 - 16a_1 a_2\left(-b_2^2 + 4b_1 b_3\right)}}{8a_1 a_2} \end{aligned} \quad (19)$$

$$\begin{aligned} \omega_2^2 &= \frac{4a_2 b_1 + 4a_1 b_3}{8a_1 a_2} + \\ &+ \frac{\sqrt{\left(-4a_2 b_1 - 4a_1 b_3\right)^2 - 16a_1 a_2\left(-b_2^2 + 4b_1 b_3\right)}}{8a_1 a_2} \end{aligned} \quad (20)$$

Each of the natural frequencies of the system corresponds to the amplitude relation of the basic form of system vibrations

$$\alpha_j = \frac{A}{B} = \frac{b_2}{2\omega_j^2 a_1 - 2b_1} = \frac{2\omega_j^2 a_2 - 2b_3}{b_2}, \quad j = 1,2 \quad (21)$$

Then the final solutions are

$$z(t) = A_1 e^{i\omega_1 t} + A_2 e^{-i\omega_1 t} + A_3 e^{i\omega_2 t} + A_4 e^{-i\omega_2 t} \quad (22)$$

$$\varphi(t) = B_1 e^{i\omega_1 t} + B_2 e^{-i\omega_1 t} + B_3 e^{i\omega_2 t} + B_4 e^{-i\omega_2 t} \quad (23)$$

After algebraic transformations and by introducing trigonometric functions and amplitude relations Eq. (21), the unknown functions of the generalized coordinates can be expressed in the following form

$$z(t) = \sum_{j=1}^{2}\left[C_j \sin(\omega_j t) + D_j \cos(\omega_j t)\right] \quad (24)$$

$$\varphi(t) = \sum_{j=1}^{2}\alpha_j\left[C_j \sin(\omega_j t) + D_j \cos(\omega_j t)\right] \quad (25)$$

Constants C_j and D_j are determined from the initial conditions

$$z(0) = z_0,\ \ \varphi(0) = \varphi_0,\ \ \dot{z}(0) = v_0,\ \ \dot{\varphi}(0) = \omega_0 \quad (26)$$

Solving the algebraic system of equations yields the constants in the following form

$$C_1 = \frac{-v_0\alpha_2 + \omega_0}{(\alpha_1 - \alpha_2)\omega_1}, \qquad C_2 = \frac{v_0\alpha_1 - \omega_0}{(\alpha_1 - \alpha_2)\omega_2}$$
$$D_1 = \frac{-z_0\alpha_2 + \varphi_0}{\alpha_1 - \alpha_2}, \qquad D_2 = \frac{z_0\alpha_1 - \varphi_0}{\alpha_1 - \alpha_2} \qquad (27)$$

By substituting constants from Eq. (27) into the expressions for the laws of vibration, Eqs. (24)-(25), we obtain the following final equations of vibration

$$z(t) = \frac{(\omega_0 - v_0\alpha_2)}{(\alpha_1 - \alpha_2)\omega_1}\sin(\omega_1 t) + \frac{(\varphi_0 - z_0\alpha_2)}{\alpha_1 - \alpha_2}\cos(\omega_1 t) + \frac{(v_0\alpha_1 - \omega_0)}{(\alpha_1 - \alpha_2)\omega_2}\sin(\omega_2 t) + \frac{(z_0\alpha_1 - \varphi_0)}{\alpha_1 - \alpha_2}\cos(\omega_2 t) \qquad (28)$$

$$\varphi(t) = \frac{\alpha_1(\omega_0 - v_0\alpha_2)}{(\alpha_1 - \alpha_2)\omega_1}\sin(\omega_1 t) + \frac{\alpha_1(\varphi_0 - z_0\alpha_2)}{\alpha_1 - \alpha_2}\cos(\omega_1 t) + \frac{\alpha_2(v_0\alpha_1 - \omega_0)}{(\alpha_1 - \alpha_2)\omega_2}\sin(\omega_2 t) + \frac{\alpha_2(z_0\alpha_1 - \varphi_0)}{\alpha_1 - \alpha_2}\cos(\omega_2 t) \qquad (29)$$

3. Forced damped vibrations of the elevating work platform with two vibrational degrees of freedom

In the case when the system shown in Fig. 2 is subjected to a random perturbing force and moment, taking into account the proportional Rayleigh-type damping, we obtain a non-homogeneous system of differential equations of a non-conservative system by applying Lagrange's equations of the second kind

$$\frac{d}{dt}\frac{\partial E_k^{(s)}}{\partial \dot z} - \frac{\partial E_k^{(s)}}{\partial z} + \frac{\partial E_p^{(s)}}{\partial z} + \frac{\partial \Phi}{\partial \dot z} = Q_z \qquad (30)$$

$$\frac{d}{dt}\frac{\partial E_k^{(s)}}{\partial \dot\varphi} - \frac{\partial E_k^{(s)}}{\partial \varphi} + \frac{\partial E_p^{(s)}}{\partial \varphi} + \frac{\partial \Phi}{\partial \dot\varphi} = Q_z \qquad (31)$$

where

$$Q_z = F(t), \qquad Q_\varphi = M(t), \qquad \delta A = Q_z\delta z + Q_\varphi\delta\varphi$$
$$\Phi = (\alpha b_1 + \beta a_1)\dot z^2 + \alpha b_2 \dot z\dot\varphi + (\alpha b_3 + \beta a_2)\dot\varphi^2 \qquad (32)$$

The virtual work δA represents the work on the virtual displacement δz from the random perturbing force $F(t)$ and $\delta\varphi$ from the random perturbing moment $M(t)$. The dissipation function Φ is formed on the basis of proportional damping with coefficients α and β. The non-homogeneous system of differential equations of the mechanical system vibrations now possesses the following form

$$2a_1\ddot z + 2(\alpha b_1 + \beta a_1)\dot z + \alpha b_2\dot\varphi + 2b_1 z + b_2\varphi = F(t) \qquad (33)$$

$$2a_2\ddot\varphi + 2(\alpha b_3 + \beta a_2)\dot\varphi + \alpha b_2\dot z + 2b_3\varphi + b_2 z = M(t) \qquad (34)$$

It is convenient to observe the coupled system of non-homogeneous differential equations using the method of modal analysis by translating the system of the generalized

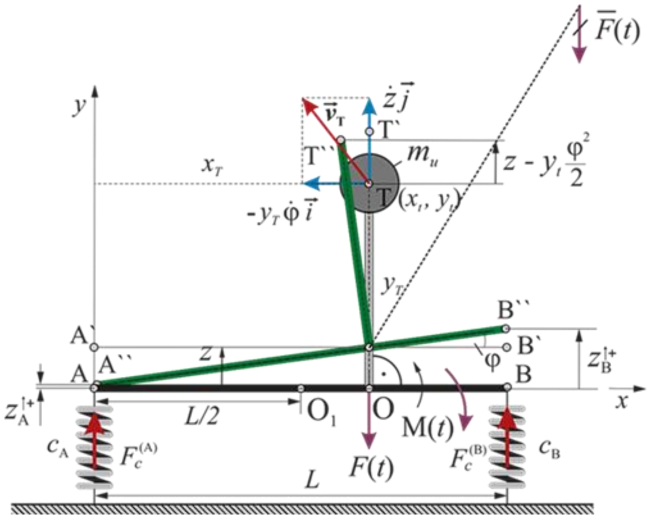

Fig. 2 Mechanical MEWP model subjected to a random perturbing force and moment

coordinates $z(t)$ and $\varphi(t)$ into the system of the main coordinates $p_1(t)$ and $p_2(t)$. In that case, it is necessary to write the system of Eqs. (33)-(34) in the matrix form

$$\begin{bmatrix} 2a_1 & 0 \\ 0 & 2a_2 \end{bmatrix}\begin{Bmatrix} \ddot z \\ \ddot\varphi \end{Bmatrix} + \begin{bmatrix} 2(\alpha b_1 + \beta a_1) & \alpha b_2 \\ \alpha b_2 & 2(\alpha b_3 + \beta a_2) \end{bmatrix}\begin{Bmatrix} \dot z \\ \dot\varphi \end{Bmatrix} + \begin{bmatrix} 2b_1 & b_2 \\ b_2 & 2b_3 \end{bmatrix}\begin{Bmatrix} z \\ \varphi \end{Bmatrix} = \begin{Bmatrix} F(t) \\ M(t) \end{Bmatrix} \qquad (35)$$

that is,

$$\mathbf{M}\ddot{\mathbf{q}} + (\alpha\mathbf{K} + \beta\mathbf{M})\dot{\mathbf{q}} + \mathbf{K}\mathbf{q} = \mathbf{F} \qquad (36)$$

The squares of the circular, eigenfrequencies of the system ω_1 and ω_2 represent the eigenvalues of the matrix $[\mathbf{M}]^{-1}[\mathbf{K}]$. The non-homogeneous system of differential equations, which corresponds to the generalized coordinates **q**, can now be translated into the system of the main coordinates **p**, i.e. $p_j(t)$, j=1,2, by introducing the modal system matrix $[\mathbf{P}]=[\{\mathbf{X}_1\}\{\mathbf{X}_2\}]$ whose columns represent the normalized basic forms of vibration

$$\{\mathbf{q}(t)\} = \sum_{j=1}^{2} p_j(t)\{\mathbf{X}_j\} \qquad (37)$$

Transformation Eq. (37) is equivalent to the linear transformation between the generalized and main system coordinates

$$\{\mathbf{q}(t)\} = [\mathbf{P}]\{\mathbf{p}(t)\} \qquad (38)$$

Substituting Eq. (38) into system Eq. (36) yields

$$\sum_{j=1}^{2}\ddot p_j(t)[\mathbf{M}]\{\mathbf{X}_j\} + \sum_{j=1}^{2}\dot p_j(t)[\alpha\mathbf{K} + \beta\mathbf{M}]\{\mathbf{X}_j\} + \sum_{j=1}^{2} p_j(t)[\mathbf{K}]\{\mathbf{X}_j\} = \{\mathbf{F}\} \qquad (39)$$

If we multiply both sides of expression Eq. (39) scalarly with $\{\mathbf{X}_r\}$ for the random r=1, 2, we obtain

$$\sum_{j=1}^{2}\ddot{p}_j(t)(\{\mathbf{X}_r\},[\mathbf{M}]\{\mathbf{X}_j\})+\sum_{j=1}^{2}\dot{p}_j(t)(\{\mathbf{X}_r\},[\mathbf{C}]\{\mathbf{X}_j\})+ \\ +\sum_{j=1}^{2}p_j(t)(\{\mathbf{X}_r\},[\mathbf{K}]\{\mathbf{X}_j\})=(\{\mathbf{X}_r\},\{\mathbf{F}\}) \tag{40}$$

By applying the orthogonality conditions of the basic forms of vibration, in each of the sums we obtain only one member, which is different from zero for $r=j$. As the basic forms of vibration are normalized, Eq. (40) gets the form

$$\ddot{p}_r(t)+2\zeta_r\omega_r\dot{p}_r(t)+\omega_r^2 p_r(t)=g_r(t),\quad r=1,2 \tag{41}$$

where $g_r(t)=(\{\mathbf{X}_r\},\{\mathbf{F}\})$ and $\zeta=(½)(\alpha\omega_r+\beta(\omega_r)^{-1})$.

The convolution integral solution of equation Eq. (41) is

$$p_r(t)=\frac{1}{\omega_r\sqrt{1-\zeta_r^2}}\int_0^t g_r(\tau)e^{-\zeta_r\omega_r(t-\tau)}\sin\left[\omega_r\sqrt{1-\zeta_r^2}(t-\tau)\right]d\tau \\ r=1,2 \tag{42}$$

By substituting the obtained solutions Eq. (42) into the transformation equation of coordinates, Eq. (37), we obtain the final system vibration equation in the form

$$\{\mathbf{q}(t)\}=\begin{Bmatrix} z(t) \\ \varphi(t) \end{Bmatrix}=\begin{Bmatrix} X_{11}(\omega_1)p_1(t)+X_{12}(\omega_2)p_2(t) \\ X_{21}(\omega_1)p_1(t)+X_{22}(\omega_2)p_2(t) \end{Bmatrix} \tag{43}$$

4. Numerical example

As the mechanical system of the elevating work platform comprises twelve mass elements connected by joints that do not allow any changes in the length between their centres of gravity during vibrations, the actual values of measured masses were reduced to the centre of gravity of the system of material points. The masses of the mechanical system elements and the coordinates of their centres of gravity are shown in Table 3, in accordance with Fig. 3.

Table 3 Masses of structural elements and coordinates of their gravity centres (MEWP CTE-Z19 model)

Element #*i*	Mass m_i (kg)	Coordinate x_i (m)	Coordinate y_i (m)
0	240	6.98	3.57
1	158.36	4.7	2.96
2	202.32	1.33	2.96
3	84.08	1.22	2.34
4	124.6	1.01	2.09
5	111.33	2.51	1.67
6	84.08	1.01	1.11
7	128.34	1.22	0.83
8	187.2	0	0
9	3650	0.72	–0.47
10	102.6	–0.27	2.48
11	20.24	0.33	0.22
12	38.2	0.83	2.34

The coordinate system, upon which these dimensions with coordinates were selected, is positioned in the gravity centre of the structural element #8 (x_{T8}, y_{T8}).

$$x_{T8}=\frac{\sum_{k=1}^{12}m_k x_k}{\sum_{k=1}^{12}m_k}=1.18\ \text{m},\quad y_{T8}=\frac{\sum_{k=1}^{12}m_k y_k}{\sum_{k=1}^{12}m_k}=0.27\ \text{m} \tag{44}$$

The entire system mass is

$$m_u=\sum_{k=1}^{12}m_k=5131.35\ \text{kg} \tag{45}$$

Taking into account the width of the platform of L=2.34 m, i.e. for the coordinate system in Fig. 1, the gravity centre of the system has the following coordinates

$$x_T=1.8238\ \text{m},\qquad y_T=0.549861\ \text{m} \tag{46}$$

By substituting the actual measured numerical values, we obtain the natural frequencies of the system

$$\omega_1=9.33\ \frac{\text{rad}}{\text{s}}=1.48\ \text{Hz} \\ \omega_2=29.96\ \frac{\text{rad}}{\text{s}}=4.76\ \text{Hz} \tag{47}$$

The rigidities of the supports are

$$c_A=c_B=\frac{9\cdot 28}{0.001}\ \frac{\text{N}}{\text{m}} \tag{48}$$

The obtained vibration periods are

$$T_1=0.672\ \text{s},\qquad T_2=0.209\ \text{s} \tag{49}$$

5. Experimental testing of the elevating work platform

The conducted experimental research into the dynamics of the elevating work platform (PUC “Gorica” Niš, 2012) determined the behaviour characteristics of the support structure in extreme and incidental situations (Radoičić 2016). The research encompassed a large number of tests performed on the CTE-Z19 machine including the measurement of stress-strain, acceleration, force, unloading time, period of vibration. In this paper particular attention is paid to the experimental determination of the period of vibration and frequencies, during free and forced vibrations of the structure.

The following equipment was used for testing: HBM MGC+ measuring signal amplifier, HBM U2A/10t force sensor, HBM LY 10/120Ω strain gauges, as well as Philips PR9369/10 acceleration sensor (Fig. 3). The mass of the test load corresponded approximately to the mass of one worker and accompanying tools in the platform basket (test load + measuring transducer = 120 kg). The work platform was operated using control instruments from the ground, without the presence of a worker on it. The testing was performed by repeating the given scenarios at several different work heights and reaches.

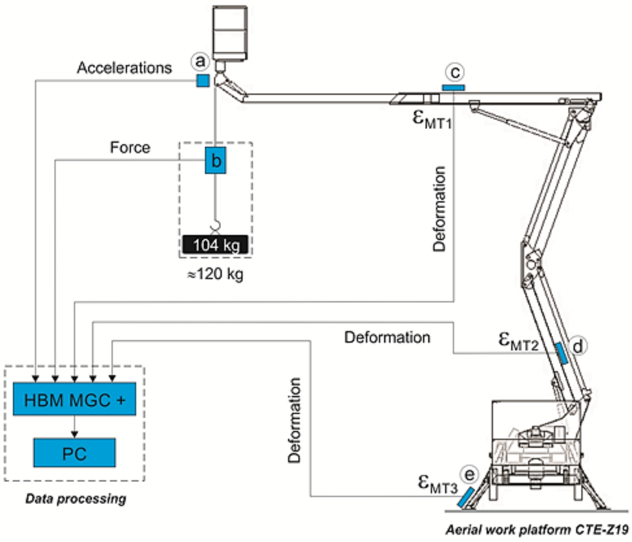

Fig. 3 Layout of the measuring equipment: a – Philips PR9369/10 acceleration sensor; b – HBM U2A/10t force transducer; c, d, e – HBM LY 10/120Ω strain gauge

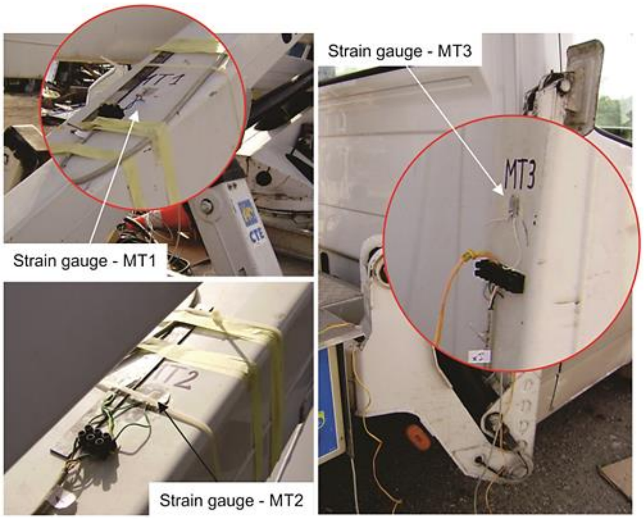

Fig. 4 Measuring points on the support structure of the platform for the measurement of the stress-strain state (MT1, MT2 and MT3 strain gauge)

5.1 Free elevating work platform vibrations

Deformations were measured using MT1 and MT2 strain gauges positioned on the third and first section of the boom (positions "c" and "d", Fig. 3), as well as MT3 strain gauge positioned on the front stabilizer ("e", Fig. 3). The measuring points were chosen with the intent to avoid the zones of concentrated strains during measuring, Fig. 4. One of the measurements (measurement no. 2) was conducted at the platform reach of 6.7 m and the work height of 5-5.5 m (i.e. 4.1 m from the ground to the basket floor). The incident scenario encompassed lifting the load (accompanied by forced vibrations with the structure coming to rest) and the excitation that caused the load (object) to fall from the platform basket. The falling of the object was simulated by breaking the rope that tied the load of 120 kg in total mass to the platform basket, Fig. 3. The results of deformation measuring were used to identify the experimental values of the vibration period.

For further analysis, we isolated the deformation values represented by MT1 curve. Figure 5 shows a detail of structural calming after the fall of the load. The first 40 amplitudes of free vibrations become sufficiently observable, which facilitates the identification of the first 39 individual periods of vibration, Fig. 5. This allows us to determine the mean experimental value of the period of vibration T_{ex}, i.e. the eigenfrequency of the structure ω_{ex} (after unloading – the fall of the load), values Eq. (50).

$$T_{ex} = \frac{1}{n}\sum_{i=1}^{n=39} T_i = 0.6974 \quad s, \quad \omega_{ex} = \frac{1}{T_{sr}} = 1.4338 \quad Hz \qquad (50)$$

After the fall of the load, the highest acceleration of the work platform in the vertical y-direction, as the dominant direction of vibrations, amounted approximately to ±0.6g, and it was measured using the "a" acceleration transducer shown in Fig. 3.

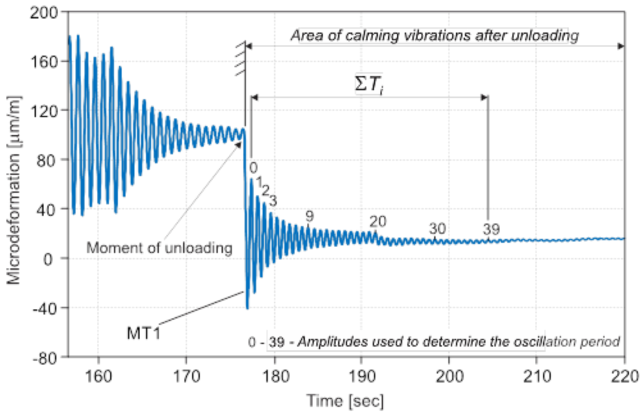

Fig. 5 Determination of the mean experimental value of the vibration period T_{ex} at free vibration (strain gauge 3)

5.2 Forced elevating work platform vibrations

Forced vibrations of the support structure were experimentally excited in the following manner: first, the work platform was raised with the load (without people); then, vibrations of the articulated-telescopic boom were calmed (led to rest) at the given work height and reach; finally, forced vibrations of the previously calmed structure were excited by a person from the ground continually and forcefully pulling the rope tied to the platform basket (simulated malicious action). The aim of this experiment was to show that any malicious action by people, caused by a relatively small perturbing force, can result in multiplied effects and significantly greater deflections of the structure, which can even lead to overturning. The period of forced vibrations $T_{ex,2}$ (due to malicious action) was determined from the diagram in Fig. 6, which shows the curve of the change in the force of the rope during the experiment (measurement no. 3). In this measurement, the work platform of the lift with the load occupied the same position as in measurement no. 2 (section 5.1). After 455th sec of measurement, the structure was subjected to a more

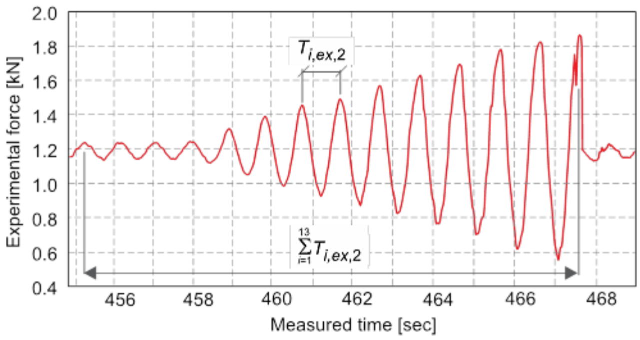

Fig. 6 Experimental identification of the period of the MEWP forced vibrations

intensive forced action, introduced by manually pulling the rope, which resulted in a gradual increase in the force amplitudes (Fig. 6). In the observed time interval, Fig. 6, the force measurement curve is characterized by a sufficient number of pure full harmonic vibrations.

On the basis of thus obtained information, the period and frequency of forced vibrations were calculated as mean values of the parameters of the dynamic behaviour of the machine in the characteristic measuring interval, Eq. (51).

This experiment with forced structural vibrations led to an increase in the dynamic force coefficient whose maximal value corresponds to the moment of reaching the highest manual (dynamic) force $F_{dyn}^{(max)}$, Eq. (52). The static force was measured in the rope in the state when the lifted load was at rest, and before the introduction of the forced action, and it amounted to F_{st}=120 kg.

$$T_{ex,2}=\frac{\sum_{i=1}^{13}T_{i,ex,2}}{13}=\frac{467.55-455.4}{13}\cong 0.93\quad \text{sec}$$
$$\Omega_{ex,2}=\frac{1}{T_{ex,2}}=1.07\quad \text{Hz} \tag{51}$$

$$K_F=\frac{F_{dyn}^{\max}}{F_{st}}\cong 1.7 \tag{52}$$

The “a” acceleration transducer (Fig. 3) was used, in the same experiment, to measure the largest acceleration of the work platform of ±1.3g in both senses of the vertical y-direction (g=9.81 m/s^2).

6. Development of the MEWP FE model

The possibilities of FEM allowed us to introduce the accurate topology of the structure and calculate the eigenvalues, structural and viscous damping, and elastic properties of the structure material. Parallel experimental testing can be of a great useful for the numerical analysis verification in the dynamic investigations of carrying structures. The examples of using FEM and SAP tools for the numerical analysis of the space steel structures, including adequate experimental support, in the papers of authors Arisoy and Erol (2018), Arslan *et al.* (2017) and Lu *et al.* (2010) are shown.

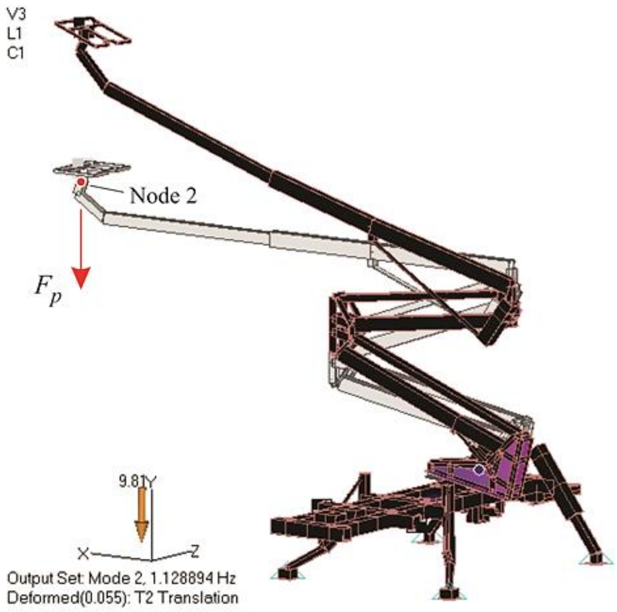

Fig. 7 Original FE model of the MEWP; the second mode shape, Ω_2=1.128894 Hz, F_p - perturbing force

The support structures of platforms are usually modelled using the BEAM finite elements (Jovanović *et al*. 2010). In this research 229 BEAM elements and 33 PLATE elements (vehicle floor sheets) were used to create a model of the elevating work platform. Special attention was paid to the description of joints in nodes (DOF) which significantly influence the idealized deformation of the linear elements of the structure. Bearing in mind that the displacement of impact force points in the nodes is not small compared with the dimensions of the elevating work platform, the FE model in Fig. 7 is adapted for nonlinear analysis. The lowest frequency of the system was determined using the Lanczos method. The basis for the analysis of natural frequencies and mode shapes in large and high frame structures can also be the Euler-Bernoulli beam theory and numerical assembly method (Sabuncu *et al.* 2016, Tan *et al.* 2017).

The analysis in this research was conducted using the PLM SIEMENS (FEMAP) software. In addition, for the purposes of such modal and dynamic analyses, the modelling of the carrying elements of large structures very often is carried out using the ANSYS software (Wu *et al.* 2017). Figure 7 shows the second mode shape of the model vibrations (the vertical direction), subjected to the perturbing force F_p.

The modelling of damping using the damping coefficient is of utmost importance for transient analysis. Damping resistances occur within the material itself (viscous damping) and inside the mechanical structure of the oscillatory system (structural damping). It is very difficult to accurately determine the influence of damping resistances on the behaviour of the structure theoretically, thus it is best to do this experimentally (Radoičić and Jovanović 2013). Such experiences were used in this research as well.

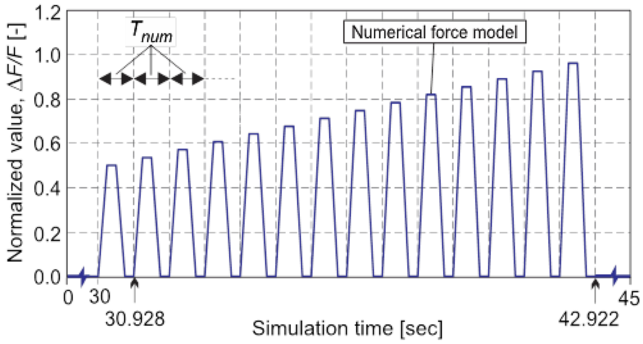

Fig. 8 Numerical excitation force of the work platform

Table 4 Comparative overview of the research results

		Investigation method		
		Experimental	Numerical	Analytical
Free vibration	Frequency ω (Hz)	1.43	1.45	1.48
	Oscillation period T (sec)	0.70	0.69	0.67
Forced vibration	Frequency Ω_2 (Hz)	1.08	1.13	
	Oscillation period T_2 (sec)	0.93	0.89	

6.1 Modelling the excitation force

The pronounced vertical vibrations of the real support structure were caused by the force of manually pulling the rope tied to the work platform. This dynamic excitation force was measured and it is presented in Fig. 6. According to that force, the numerical form of excitation was first defined and then applied in transient analyses of the FE model of the elevating work platform.

The excitation force was modelled in the form of a repeated impulse function of growing intensity, with the impulse units, 14 of them, possessing the trapezoidal shape, Fig. 8. The modelling was performed in the PLM SIEMENS software. The same number of manually generated and measured impulses (cycles) can be seen in Fig. 6. To model the numerical impulse function of the excitation we used the experimentally obtained value of the forced vibration period. Thus the step of the numerical function of the force in Fig. 8 was defined, i.e.

$$T_{num} = 0.928 \quad \text{sec} \quad \left(\cong T_{ex,2}\right) \tag{53}$$

7. Comparative accuracy analysis

A comparative overview of the analysis results is given in Table 4, in the form of frequencies and periods of vibration of the mobile elevating work platform system. Two cases of vibrations were observed, free and forced.

Based on Table 4, the relative deviations of the results were calculated, ε%, and they are presented in Table 5. By comparing the numerical and analytical results of vibration frequencies and periods with the measured quantities, it can

Table 5 Relative deviations of the results, ε (%)

		Compared to*		
		N-E	A-E	A-N
Free vibration	Frequency ω (Hz)	1.40 %	3.50 %	2.07 %
	Oscillation period T (sec)	-1.43 %	-4.29 %	-2.90 %
Forced vibration	Frequency Ω_2 (Hz)	4.63 %		
	Oscillation period T_2 (sec)	-4.30 %		

*N-E numerical compared to experimental, A-E analytical compared to experimental, A-N analytical compared to numerical

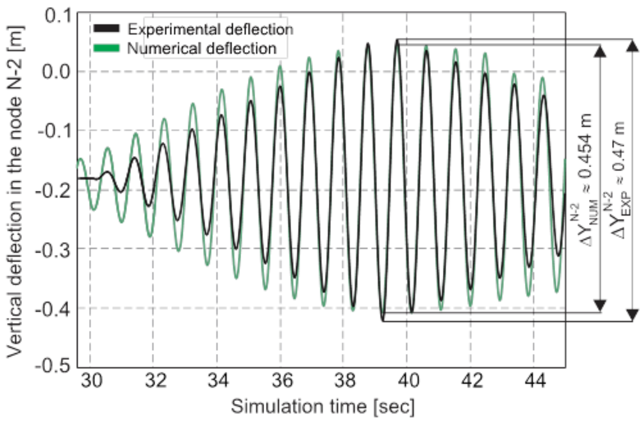

Fig. 9 Comparative overview of the measured and numerically obtained deflection under the influence of the perturbing force

be concluded that the analytical and numerical FE model of the platform possesses the accuracy with the deviation of ε <5% (Table 5).

The proof of the quality of the FE platform model can be observed in Fig. 9, where diagrams are employed to comparatively present the vibration amplitudes of the support structure obtained from the numerical simulation and the experiment. The curve of the numerical change in the deflection of the boom end (work platform) in the vertical *y*-direction is shown in lighter colour, while the curve obtained experimentally is shown in darker colour. What is evident is the phase agreement of forced vibrations and a small relative deviation of the values of maximal amplitudes of 3.4%, with the total maximal numerical displacement (ΔY_{NUM}) being somewhat smaller than the experimental one (ΔY_{EXP}). The reason behind the deviation in the results lies in the deflection of the amplitude envelope function that depends on the calming time of the basket and the load.

The relative deviation of the numerical values of the deflection can be reduced by fine-tuning the total structural damping coefficient *G* before transient analysis. The forced vibration frequency is not constant during the action of the perturbing force, since the force intensity and the speed of manually pulling the rope are not always the same during the experiment. As part of the numerical analyses, the approximation was also performed by adopting the mean frequency value, which led to smaller deviations in the analysis results.

8. Conclusions

The observed oscillatory problems are commonly present in the engineering practice (mechanical engineering, civil engineering, aeronautical industry). It becomes very important to obtain the best possible solution approximations when analysing the vibrations of complex dynamic systems. One type of complex dynamic systems, analysed in this paper, includes vibration systems of mobile elevating work platforms. From the standpoint of the applied theory of vibration, such a problem occupies an important place in the analyses of mechanical systems with a large number of cyclic operations and excitations that can lead to resonance.

Circular frequency is the basic quantity of a mechanical oscillatory system linked to its nature. The theoretical determination of frequencies of a mechanical system aims to facilitate the experimental analysis of the problem from the perspective of determining the law of vibration using the given final equations of motion. Such an analytical procedure, resulting in the laws of vibration, allows for a detailed insight into the dynamic behaviour of a system subjected to its physical parameters. In this way, it is possible to discuss the motion on the basis of the changes in the basic physical system parameters, which is not easy to do numerically or experimentally. In that case, if there is an analytical solution that corresponds to the mechanical model being analysed, it is possible to conduct a numerical or experimental analysis to verify the obtained analytical results.

Every actual problem of complex dynamic structures has to contain certain idealizations and simplifications that can lead to possible analytical solutions. By including the characteristic influences through rigidity, damping and perturbing force of the system, it is possible, from the standpoint of the theory of vibration, to reach the conclusions on the behaviour of a system as a dynamic absorber. The behaviour of a system as a dynamic absorber represents the basic problem of systems with two vibrational degrees of freedom, and as such it was analysed in this paper. In such cases, on the basis of the known parameters of the perturbing force (amplitudes and forced frequencies) one can stabilize a system at the point of its direct excitation by changing the masses and rigidity of the basic system. Thus the oscillatory motion can be directed towards the system element that is already known as being capable of safely withstanding the displacements of high amplitudes with appropriate frequencies.

As the basis for further analysis of the behaviour of systems, as dynamic absorbers, it is necessary to perform the mathematical analysis presented in this paper. Furthermore, from the standpoint of mechanics, numerical and experimental testing of analytical results is of special importance because it provides a global insight into the system behaviour, while the dynamic analysis of the problem receives its necessary verification. Every possible change in the system parameters consequently leads to a change in the system motion, which can be determined and used to predict a scenario from the safety perspective, as well as the perspective of preserving the structure from fracture and damage.

Acknowledgments

This paper is part of the project TR-35049 at the University of Niš, Faculty of Mechanical Engineering, and is financially supported by the Ministry of Education, Science and Technological Development of the Republic of Serbia.

References

Arisoy, B. and Erol, O. (2018), "Finite element model calibration of a steel railway bridge via ambient vibration test", *Steel Comp. Str.*, **27**(3), 327-335. https://doi.org/10.12989/scs.2018.27.3.327.

Arslan, G., Sevim, B. and Bekiroglu, S. (2017), "Determination of structural performance of 3D steel pipe rack suspended scaffolding systems", *Str. Eng. Mech*., **64**(5), 671-681. https://doi.org/10.12989/sem.2017.64.5.671.

Bošnjak, S., Gnjatović, N., Momčilović, D., Milenović, I. and Gašić, V. (2015), "Failure analysis of the mobile elevating work platform", *Case Studies Eng. Failure Analysis*, **3**, 80-87. https://doi.org/10.1016/j.csefa.2015.03.005.

Bošnjak, S., Zrnić, N. and Dragović, B. (2009), "Dynamic response of mobile elevating work platform under wind excitation", *Strojniški vestnik – J. Mech. Eng.*, **55**(2), 104-113.

Dong, R., Pan, C., Hartsell, J., Welcome, D., Lutz, T., Brumfield, A., Harris, J., Wu, J., Wimer, B., Mucino, V. and Means, K. (2012), "An investigation on the dynamic stability of scissor lift", *Open J. Safety Science Tech.*, **2**(1), 8-15. http://dx.doi.org/10.4236/ojsst.2012.21002.

Fujioka, D., Rauch, A. and Singhose, W. (2009), "Tip-over stability analysis of mobile boom cranes with double-pendulum payloads", *American Control Conference*, St. Louis, USA, June.

HBM (Hottinger Baldwin Messtechnik GmbH) (2012), "HBM Data sheets", Im Tiefen See 45, 64293 Darmstadt, Germany, https://www.hbm.com/en.

Jovanović, M. (1990), "Optimization of the level-luffing system structure and resistance of the mechanism of portal-rotating cranes", Ph.D. Dissertation, University of Niš, Faculty of Mechanical Engineering, Niš, Serbia.

Jovanović, M., Milić, P., Janošević, D. and Petrović, G. (2010), "Accuracy of FEM analyses in function of finite element type selection", *Facta Universitatis - Series Mech. Eng.*, **8**(1), 1-8. https://scindeks.ceon.rs/article.aspx?artid=0354-20251001001J.

Leah, C., Riley, D. and Jones, A. (2013), "Mobile Elevated Work Platform (MEWP) incident analysis", Research report RR961; The Health and Safety Laboratory/Health and Safety Executive, Buxton, United Kingdom. http://www.hse.gov.uk/research/rrpdf/rr961.pdf.

Lu, P., Zhao, R. and Zhang, J. (2010), "Experimental and finite element studies of special-shape arch bridge for self-balance", *Str. Eng. Mech*., **35**(1), 37-52. https://doi.org/10.12989/sem.2010.35.1.037.

Radoičić G. (2016), "The dynamical behaviour of certain classes of heavy lifting and construction machinery from the aspect of accidental events", Ph.D. Dissertation, University of Niš, Faculty of Mechanical Engineering, Niš, Serbia.

Radoičić, G. (2006), "The vibro-comfort testing on a mobile elevating work platform", *J. Applied Eng. Science*, **11**(-), 25-34.

Radoičić, G. and Jovanović, M. (2013), "Experimental identification of overall structural damping of system", *Strojniški vestnik – J. Mech. Eng.*, **59**(4), 260-268. https://doi.org/10.5545/sv-jme.2012.569.

Radoičić, G. and Jovanović, M. (2017), "Transient simulation of impulse wind effect on a tall shipyard frame structure", *Int. J. Applied Eng. Science*, **15**(2), 192-202. https://doi.org/10.5937/jaes15-12935.

Radoičić, G., Jovanović, M. and Marinković, D. (2014), "Non-linear incidental dynamics of frame structures", *Str. Eng. Mech.*, **52**(6), 1193-1208. https://doi.org/10.12989/sem.2014.52.6.1193.

Rašković, D. (1965), *Theory of Oscillations*, Scientific Book (Naučna knjiga), Belgrade, Serbia.

Sabuncu, M., Ozturk, H. and Yashar, A. (2016), "Static and dynamic stability of cracked multi-storey steel frames", *Str. Eng. Mech.*, **58**(1), 103-119. https://doi.org/10.12989/sem.2016.58.1.103.

Stojanović, V. and Kozić, P. (2015), *Vibrations and Stability of Complex Beam Systems*, Springer International Publishing, Switzerland.

Tan, G., Wang, W., Jiao Y. and Wei, Z. (2017), "Free vibration analysis of continuous bridge under the vehicles", *Str. Eng. Mech.*, **61**(3), 335-345. https://doi.org/10.12989/sem.2017.61.3.335.

Wu, X. and Li, H. (2017), "Experimental and analytical behaviour of a pre-stressed U-shaped girder bridge", *Str. Eng. Mech.*, **61**(3), 427-436. https://doi.org/10.12989/sem.2017.61.3.427.

CC